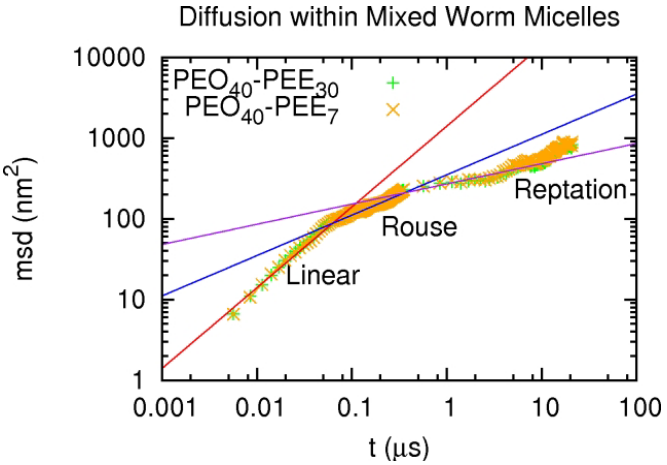

Sup. Fig. A. Mean squared displacement (msd) of PEO_{40}-PEE_{32} and PEO_{40}-PEE_7 diblocks in the 30% PEO_{40}-PEE_7 worm micelle system. The different scaling regimes are identified: linear (t), Rouse ($t^{1/2}$), and reptation ($t^{1/4}$). The overlap between the PEO_{40}-PEE_{32} and PEO_{40}-PEE_7 data sets suggests that activated reptation is occurring, namely, the diffusion of the copolymer is dictated by the PEO.

In order to assess the timescales of the lateral diffusion of the polymer chains, the mean squared displacement (msd) of the interfacial beads was measured for both diblocks in the worm micelle in the 30 mol% metastable worm. Analysis shows that the diffusion of copolymer chains over time, as shown in Sup. Fig. A., is consistent with ballistic (t), Rouse ($t^{1/2}$), and reptation ($t^{1/4}$) dynamics found in a polymer melt[43,44]. After ter 10μs, another relaxation time period has been reached. After the $t^{1/2}$ scaling regime, the $t^{1/4}$ scaling regime appears again in polymer theory after the Rouse relaxation time, τ_R, for polymer melts. The latter reptation dynamics has been confirmed for longer copolymers, whose segments are greater than their entanglement weights[45]. The Rouse time, and thereafter, corresponds to a mean squared displacement of approximately 10-20nm, which is significant lateral diffusion for a cylindrical micelle of length 50 nm, and greater than the micelle radius (~5nm). This implies that the lateral displacement of the chains is of comparable timescales to micelle break-up.

Most noticeably, the slope of the diffusion is independent of copolymer length in the Rouse and reptation regimes (Fig. 5),

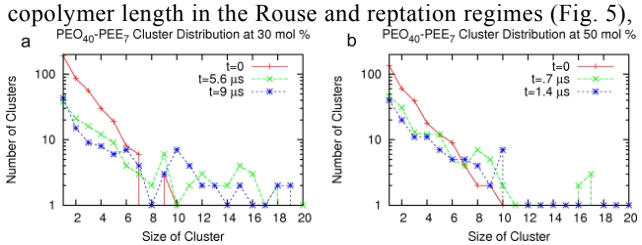

Sup. Fig. B. Cluster size distributions. Aggregation of PEO_{40}-PEE_7 over time in systems of a) 30 mol % PEO_{40}-PEE_7 and b) 50 mol% PEO_{40}-PEE_7. The 30 mol% system shows the formation of a bimodal distribution with a peak at cluster sizes of ~10, this is indicative of a local demixing. This distribution does not significantly change during the rest of the simulation. The 50 mol% system does not show this peak in the distribution, except during relatively small timescale fluctuations.

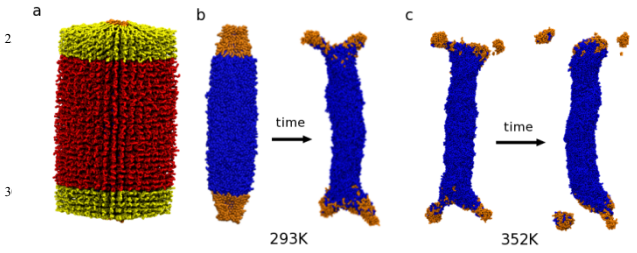

Sup. Fig. C. Extrapolation to extreme segregation. 30 mol% of PEO_{40}-PEE_7 are initially placed at the start of the simulation at the two endcaps. From left to right, a) shows the corona, while b) illustrates the core. With time, this significantly disrupts the worm micelle structure. The core forms buds at the ends. c) At high temperatures (352K), this results in pinch-off of small spherical micelles, composed almost entirely of PEO_{40}-PEE_7.

which suggests activated reptation[46,47]. An activated mechanism of chain diffusion is proposed for lamellar block copolymers, with the barrier dependent on the degree of interfacial segregation[45]. Here, it is clear the activation mechanism is limited by the longest block and is dominated by the hydrophilic PEO, which has the same length for both of the diblocks forming the micelle. The entanglement molecular weight of PEE at room temperature of ~ 104 monomers is much longer than the length of the hydrophobic tails[46]. At 353 K, the entanglement molecular weight of PEO ~ 44 monomers[46], which is approximately the length of the hydrophilic PEO in our simulations, and thus is just long enough to display entanglement behavior.

Sup. Fig B. show sthat for the 30 mol % concentration of PEO_{40}-PEE_7, there is a localized demixing and clusterization that develops over time, of copolymer clusters of PEO_{40}-PEE_7 within the core > 10. This localized aggregation is not seen in the higher mol %'s preceding, during, or post break-up of the worm-micelle, except during relatively small timescale fluctuations. Previously, we considered a random distribution of PEO_{40}-PEE_7 copolymers dispersed within the originally stable worm micelle. Now, we consider the case of a heterogeneous distribution. We start with 30 mol % of PEO_{40}-PEE_7 copolymers at opposite ends of the worm, and find that this significantly disrupts the worm micelle structure. We see that the core forms buds at the ends with time, almost entirely composed of the short PEO_{40}-PEE_7 (Supplementary Fig. C). At elevated temperatures (352 K), this results in pinch-off of small spherical micelles, composed almost in entirety of PEO_{40}-PEE_7.

With longer molecular weight copolymers, a region in the phase diagram exists with higher concentration of branching and junction formation in conjunction with cylindrical micelles4. Analysis performed by May et al. indicate that these intermicellar junctions, possibly formed through micellar fusion, are energetically metastable48. They are strongly dependent on the kinetics, history, the strength of the coupling between the preferred curvature of each polymer component and the curvature of the micellar surface. For lipids, it is found that the stronger the asymmetry of the lipid, the stronger the coupling, between two layers in a vesicle 12.

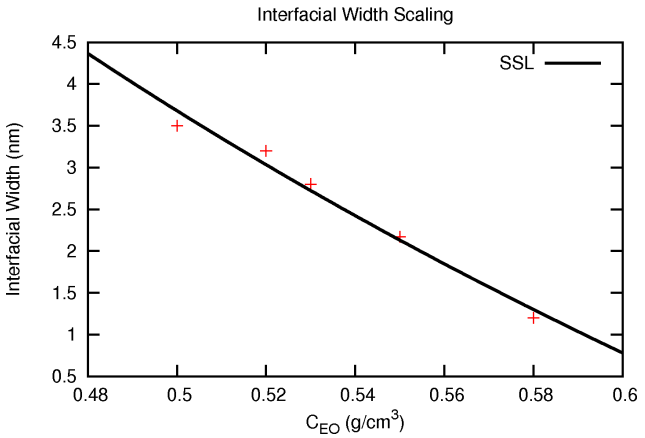

Sup. Fig. D. Scaling of interfacial width, w, of Fig. 2 in the main text, with concentration of PEO, C_{EO}. An increase in polymer length leads to swelling of the corona and a decrease in C_{EO}. The strong segregation limit (SSL) predicts $w \sim C_{EO}^{-0.5}$.

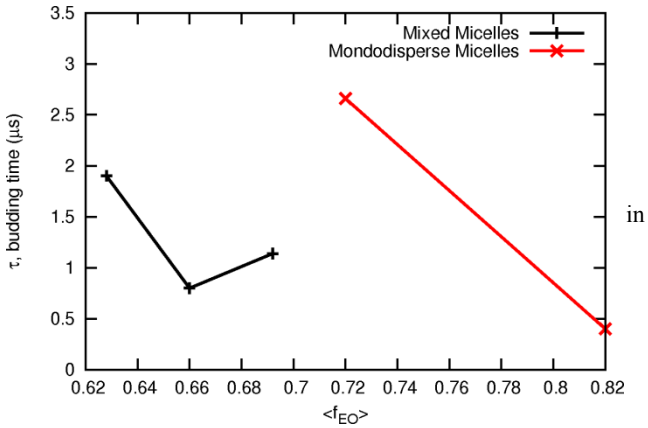

Sup. Fig. E. τ, budding time of kinetically unstable worm micelle for mixed and monodisperse micelles, as a function of <f_{EO}>, Eq. 3 in the text. The mixed micelles exhibit faster timescales to the first bud formation and subsequent break-up.

For example, for even longer copolymers, with shortening and degradation, a higher degree of asymmetry between the components is possible, and thus, stronger coupling with curvature.

In Sup. Fig. E. we plot the life-time of the micelle to first bud formation vs. the average hydrophilic block fraction, <f_{EO}>, defined by Eqn. 3 in the text. We see that with increased <f_{EO}>, breakup time decreases. In comparison between the single-component, and multi-component micelles, we find that the breakup time decreases for multi-component micelles, illustrating further that complex molecular processes, such as interfacial curvature effects, may promote this budding and break-up.

Mixed Micelles (Concentration of PEO_{40}-PEE_7 (f_{EO} = 0.82) in a PEO_{40}-PEE_{32} worm)	Simulation Size (N_{total})	Micelle lifetime **(until initial budding and pinch)**	Total Simulation Time
30%	1,160,000	Stable	40.0 μs
40%	1,156,000	1.9 μs	8.8 μs
50%	1,153,000	0.8 μs	8.8 μs
60%	1,150,000	1.14 μs **	8.8 μs

Monodisperse Polymer Lengths (f_{EO} Concentration)	Simulation Size (N_{total})	Micelle lifetime **(until initial budding and pinch)**	Total Simulation Time
PEO_{40}-PEE_{32} (.50)	1,127,000	Stable	21.1 μs
		Stable	21.1 μs
PEO_{40}-PEE_{22} (.59)	1,131,000	5 breakup * (*average*	8.8 μs
PEO_{40}-PEE_{12} (.72)	1,134,000	2.66 μs)	21.1 μs
		1 stable breakup (400 ns)	3.5 μs
PEO_{40}-PEE_7 (.82)	1,136,000		

Sup. Table 1. Summary of worm simulations to analyze kinetic stability of monodisperse and mixed worm micelles, including micelle lifetime and total simulation time. N_{total} refers to the total number of DPD beads per simulation box. Each micelle contained 1320 polymers. *5 micelles break-up, one is stable for much longer times. Of these five, one exhibits an entangled micelle (dumbbell). **This break-up exhibits double bud formation from one end, that simultaneously bud.

Notes and references

43 P. G. de Gennes, *Scaling Concepts in Polymer Physics*. Cornell University Press, 1979.

44 M. Doi & S. F. Edwards, *Theory of Polymer Dynamics*. Oxford University Press, Oxford, 1986.

45 J. C. M. Lee, M. Santore, F. S. Bates. & D. E. Discher, *Macromolecules,* 2002, **35**, 323-326.

46 A. N. Semenov & M. Rubinstein, *European Physical Journal B,* 1998, **1**, 87-94.

47 T. P. Lodge & M. C. Dalvi, *Physical Review Letters,* 1995, **75**, 657-660.

48 S. May, Y. Bohbot & A. Ben-Shaul, *Journal of Physical Chemistry B,* 1997, **101**, 8648-8657.